Nanoscale Spin-State Ordering in LaCoO$_3$ Epitaxial Thin Films

Ji-Hwan Kwon[1,2,3], Woo Seok Choi[4,5], Young-Kyun Kwon[6], Ranju Jung[7], Jian-Min Zuo[3], Ho Nyung Lee[4] and Miyoung Kim[1,2*]

[1] Center for Correlated Electron Systems, Institute for Basic Science (IBS), Seoul 151-747, Republic of Korea

[2] Department of Materials Science and Engineering and Research Institute of Advanced Materials, Seoul National University, Seoul 151-744, Republic of Korea

[3] Department of Materials Science and Engineering and Frederick Seitz Materials Research Laboratory, University of Illinois at Urbana−Champaign Urbana, Illinois 61801, United States

[4] Materials Science and Technology Division, Oak Ridge National Laboratory Oak Ridge, Tennessee 37831, United States

[5] Department of Physics, Sungkyunkwan University Suwon 440-746, Republic of Korea

[6] Department of Physics and Research Institute for Basic Sciences, Kyung Hee University Seoul 130-701, Korea

[7] Department of Electrophysics, Kwangwoon University Seoul 139-701, Republic of Korea

1. Two-Dimensional Spin-Ordering in LaCoO₃ Thin Films

The structural relaxation by spin ordering is 1-dimensional (1-D), whereas thin films are 2-dimensional (2-D). Two directions that are crystallographically equivalent relax in the same way; thus, we examined two transmission electron microscopy (TEM) samples that were cut perpendicular to each other (along the [100] and [010] directions). Indeed, dark stripe patterns were observed in both samples, indicating that spin ordering occurred in two dimensions in the LaCoO₃ thin films. We believe that the dark stripe pattern forms as a domain and propagates along the [100] or [010] direction. Note that there were some areas without stripes, which is assigned to the domain that had relaxed perpendicularly; the stripe pattern propagated along the electron beam direction. It is worth noting that some structural dislocations were observed only in the stripe-free domains, as shown in Fig. S1. Many of the dark-stripe-patterned domains were observed over the 100-nm width of the thin films, a value much larger than the typical TEM sampling of a few tens of nanometers. Based on these observations, we constructed a 2-D spin-ordering model, where two types of orthogonal domains of equivalent crystallographic directions form, as illustrated in Fig. S2 (randomly distributed in size and position).
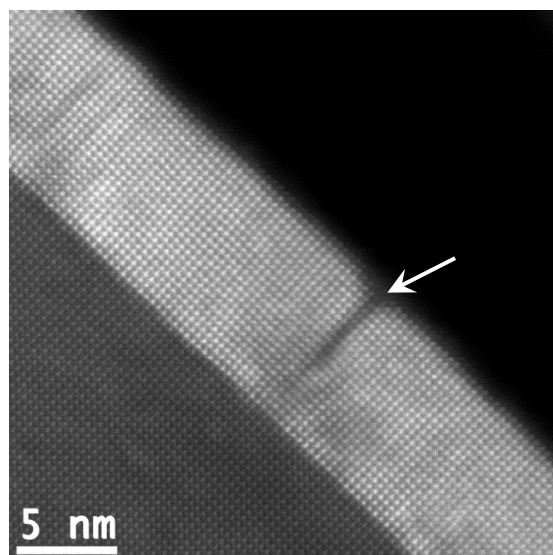
Fig. S1. High-resolution scanning transmission electron microscopy (STEM) image of LaCoO₃ thin films. No dark stripes were evident; however, dislocations were observed in these regions.
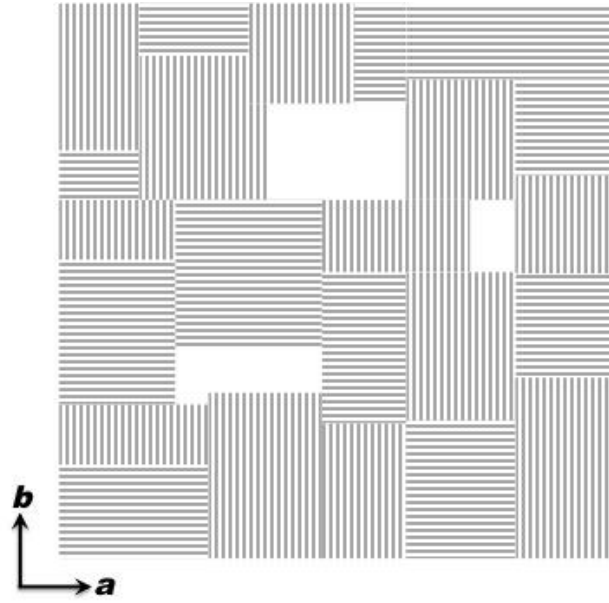
Fig. S2. Schematic diagram of the spin-ordering propagation model (dark stripe pattern) in two dimensions in LaCoO$_3$ thin films. The few areas where no dark stripe pattern was observed corresponded to relaxation via dislocations.

2. Determination of Stoichiometry

Striped patterns frequently appear in many oxides and are often associated with ordered oxygen vacancies. For example, oxygen vacancies and their ordering have been considered as the origin of lattice expansion and are related to the dark stripe pattern observed in scanning transmission electron microscopy (STEM) images in Sr-doped and oxygen-deficient LaCoO$_{3-\delta}$.[1,2] Therefore, we carefully examined the possibility of the existence of oxygen vacancies in the striped patterns. The striped patterns appearing every three unit cells imply a high density of oxygen deficiencies (~11%), which should be easily detected by X-ray absorption spectroscopy (XAS) and/or spectroscopic ellipsometry. However, previous results indicated that the LaCoO$_3$ thin films had good stoichiometry, with no discernible oxygen vacancies.

X-ray Absorption Measurements

In LaCoO$_{3-\delta}$, oxygen deficiency leads to the formation of Co^{2+}, which is characterized as a distinctive prepeak before the Co L_3 edge.[3] Our previous study showed that Co^{2+} was < 5% of the total signal, which corresponded to an oxygen deficiency of $\delta < 0.024$.[4] Recently, we performed XAS experiments with soft X-rays at the 2A undulator beamline of the Pohang Light Source (PLS); here, the total energy resolution was ~150 meV at room temperature. The Co L edge spectra were collected using the total electron yield mode. Note that due to the short probing depth of the secondary electrons, the total electron yield mode is more surface-sensitive than the fluorescence yield mode used to obtain the previous absorption spectra.[4] As shown in Fig. S3, the Co L edge spectra show no discernible prepeak before Co L_3 edge, indicating the good stoichiometry of the LaCoO$_3$ thin films. In addition, The Co L edge in the XAS spectra at room temperature and at the temperature of liquid nitrogen was almost the same each other, which is consistent with previous report of Co L edge in bulk LaCoO$_3$.[3] On the basis of spectroscopic analysis, we concluded that oxygen vacancies were not the main cause of the stripe pattern in LaCoO$_3$ thin films.
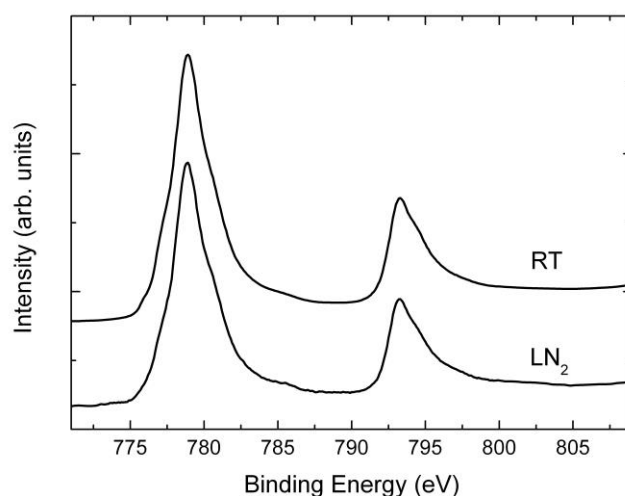

Fig. S3. Co L edge of LaCoO$_3$ thin films.

Integrated Intensity Ratio of Co *L₃/L₂* **in Electron Energy Loss Spectroscopy (EELS)**

The electron energy loss near the edge structure is sensitive to local coordinates. Specifically, the Co *L₃/L₂* edge ratio of $LaCoO_3$ is sensitive to the oxygen stoichiometry.[5–7] The integrated intensity ratio of the Co *L₃/L₂* edge was calculated using the second derivative method.[8] The bright layer and dark layer ratios were 3.46 ± 0.61 and 3.48 ± 0.48, respectively, indicating that the local Co valence did not change over the dark stripe pattern.

Partial Oxygen Deficiency in the Dark Stripe Column

The possibility of partial oxygen deficiency in the dark stripe column was tested with density functional theory (DFT) calculations. Figure S4 shows a schematic diagram of a $3 \times 3 \times 1$ supercell structure, where only one oxygen atom was deficient in the dark stripe column in the unit cell; this corresponded to an oxygen deficiency of ~4%, within the detection limit of XAS and/or spectroscopic ellipsometry. After structural relaxation, the atomic distance between La atoms was calculated to be 4.05 Å in the dark stripe column and 3.90 Å in the bright column, which was not consistent with experimental results. Although, the lattice expansion increased as the concentration of oxygen vacancies increased (with an ordered oxygen vacancy of ~11% oxygen deficiency, the calculated distance between the La atoms was ~4.25 Å); the large density of oxygen deficiencies was inconsistent with the XAS, ellipsometry, and EELS experimental results. This calculation strongly suggests that the dark stripe pattern was primarily associated with spin ordering; the contribution of the oxygen vacancies to the lattice expansion was negligible in the low-oxygen-vacancy regime.
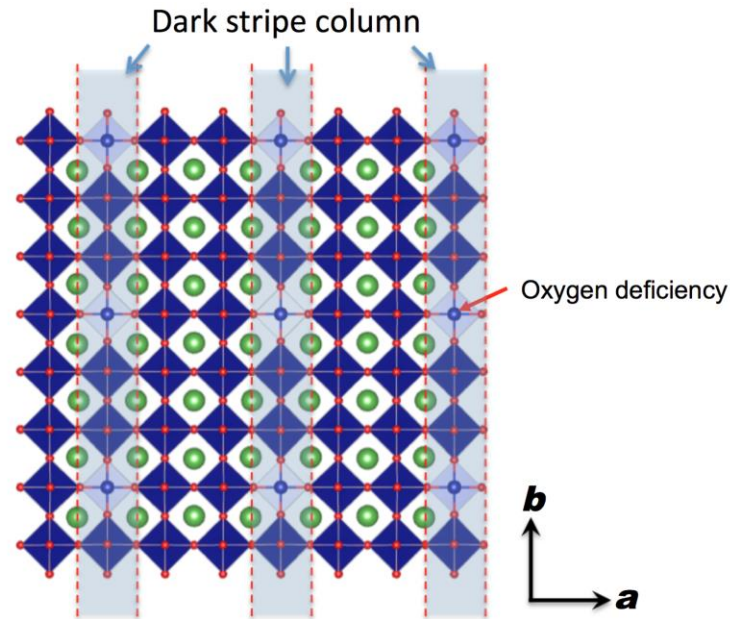
Fig. S4. Schematic diagram of the $3 \times 3 \times 1$ supercell structure of LaCoO$_3$ with one oxygen vacancy and the dark stripe column. This schematic drawing shows the in-plane atomic configuration and is expanded by two in each direction.

3. EELS Simulation

We have performed EELS simulation based on DFT calculation. The relaxed atomic structure (HLL spin configuration) via VASP was employed for EELS simulation using Wien2k software. One core hole was accounted in the O $1s$ in the 'H' state and 'L' state, respectively. Although, there is discrepancy in relative peak intensity between experimental result and simulation, which might be attributed to the complex electronic structure and limit of DFT for calculating excited state, three major peaks are clearly shown. As shown in Fig.S5, peak a in 'H' state (higher spin layer) is significantly reduced compared to that in 'L' state (low spin layer), which is consistent with our experimental result. However, we could not observed significant changes in peak c, which was markedly decreased in experiment.
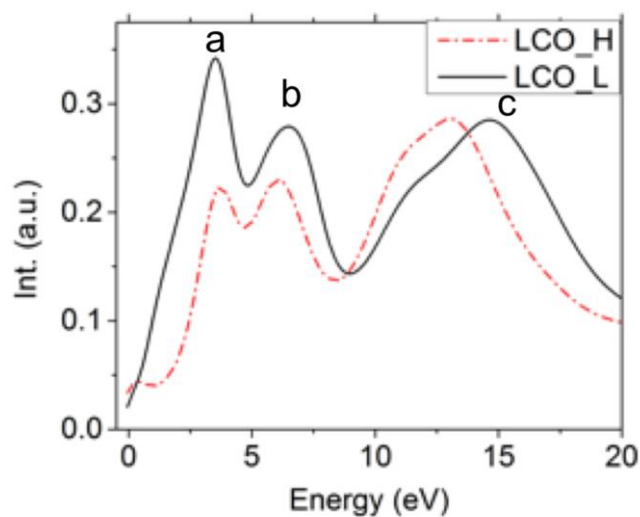
Fig. S5. Simulated O *K* edge for bright (L) and dark layer (H)

4. STEM Simulation

HAADF-STEM simulation was performed using multislice algorithm. HAADF intensity due to thermal diffuse scattering (TDS) is calculated from the absorptive potential.[9] The simulation carried out based on the experimentally measured structure. The thickness was assumed to be as 50 nm. The inner cut-off angle is 100 mrad, Cs = 1.0 mm. It clearly shows that the contrast has been reduced in the layer where La−La distance is enlarged.
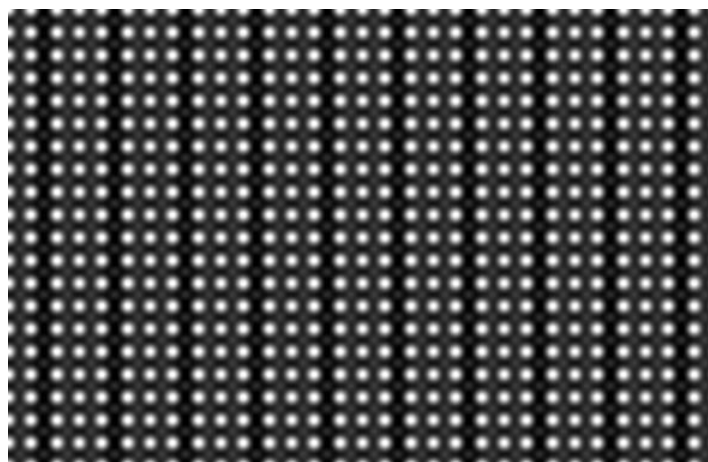

Fig. S6. Simulated HAADF-STEM image

5. Strain and Spin Configuration

The magnetic moment of Co ion (μ_B/Co) in the H layer increases as it goes from HHH to HLL configuration (Table 1), which accompanies increasing lattice constant of H layer (Fig. 3). As mentioned earlier, the ionic radius of Co^{3+}, equivalently Co−O distance increases as the spin state of Co changes from LS to HS. In our calculation, since the in-plane lattice parameter of 3 × 1 slab is fixed at that of $SrTiO_3$ substrate, the lattice constant of H layer in HHH and HHL configuration cannot be expanded as large as HLL configuration while atomic relaxation in DFT calculation. Consequently, H layer in HHH and HHL have less magnetic moment of Co ion compared to that in HLL configuration.

References

(1)   Gazquez, J.; Luo, W.; Oxley, M. P.; Prange, M.; Torija, M. A.; M, S.; Leighton, C.; Pantelides, S. T.; Pennycook, S. J.; Varela, M. *Nano Lett.* **2011**, *11*, 973.

(2)   Kim, Y. M.; He, J.; Biegalski, M. D.; Ambaye, H.; Lauter, V.; Christen, H. M.; Pantelides, S. T.; Pennycook, S. J.; Kalinin, S. V.; Borisevich, A. Y. *Nat. Mater.* **2012**, *11*, 1−7.

(3)   Abbate, M.; Fuggle, J. C.; Fujimori, A.; Tjeng, L. H.; Chen, C. T.; Potze, R.; Sawatzky, G. A.; Eisaki, H.; Uchida, S. *Phys. Rev. B* **1993**, *47*, 16124.

(4)   Choi, W. S.; Kwon, J.-H.; Jeen, H.; Hamann-Borrero, J. E.; Radi, A.; Macke, S.; Sutarto, R.; He, F.; Sawatzky, G. A.; Hinkov, V.; Kim, M.; Lee, H. N. *Nano Lett.* **2012**, *12*, 4966–4970.

(5)   Wang, Z. L.; Bentley, J.; Evans, N. D. *Micron* **2000**, *31*, 355–362.

(6)   Ito, Y.; Klie, R. F.; Browning, N. D.; Mazanec, T. J. *J. Am. Chem. Soc.* **2002**, *85*, 969–976.

(7)   Riedl, T.; Gemming, T.; Wetzig, K. *Ultramicroscopy* **2006**, *106*, 284–291.

(8)   Botton, G. A.; Appel, C. C.; Horsewell, A.; Stobbs, W. M. *Journal of Microscopy* **1995**, *180*, 211–216.

(9)   Ishizuka, K. *Ultramicroscopy* **2002**, *90*, 71–83.